
HMFS: HYBRID MASKING FOR FEW-SHOT SEGMENTATION

Seonghyeon Moon
Rutgers University
USA
sm2062@rutgers.edu

Samuel S. Sohn
Rutgers University
USA
samuel.sohn@rutgers.edu

Honglu Zhou
Rutgers University
USA
honglu.zhou@rutgers.edu

Sejong Yoon
The College of New Jersey
USA
yoons@tncj.edu

Vladimir Pavlovic
Rutgers University
USA
vladimir@rutgers.edu

Muhammad Haris Khan
Muhammad Bin Zayed University of Artificial Intelligence
UAE
muhammad.haris@mbzuai.ac.ae

Mubbasir Kapadia
Rutgers University
USA
mubbasir.kapadia@rutgers.edu

ABSTRACT

We study few-shot semantic segmentation that aims to segment a target object from a query image when provided with a few annotated support images of the target class. Several recent methods resort to a feature masking (FM) technique, introduced by [1], to discard irrelevant feature activations to facilitate reliable segmentation mask prediction. A fundamental limitation of FM is the inability to preserve the fine-grained spatial details that affect the accuracy of segmentation mask, especially for small target objects. In this paper, we develop a simple, effective, and efficient approach to enhance feature masking (FM). We dub the enhanced FM as hybrid masking (HM). Specifically, we compensate for the loss of fine-grained spatial details in FM technique by investigating and leveraging a complementary basic input masking method [2]. To validate the effectiveness of HM, we instantiate it into a strong baseline [3], and coin the resulting framework as HMFS. Experimental results on three publicly available benchmarks reveal that HMFS outperforms the current state-of-the-art methods by visible margins.

Keywords few-shot segmentation, semantic segmentation, few-shot learning

1 Introduction

Deep convolutional neural networks (DCNNs) have enabled remarkable progress in various important computer vision tasks, such as image recognition [4, 5, 6, 7], object detection [8, 9, 10], and semantic segmentation [11, 12, 13]. Albeit displaying effectiveness, DCNNs, require a large amount of labelled training data, which is quite cumbersome and costly to acquire for dense prediction tasks, such as semantic segmentation. Semi-supervised segmentation [14, 15, 16] is an alternative to this limitation, however, it still relies on a lot of weakly-labeled data for training. These models show poor generalization to unseen classes. To counter the aforementioned problems, few shot segmentation methods, that rely on a few annotated support images, have been actively studied [17, 18, 19, 20, 21, 22, 23, 24, 25, 26, 27, 1, 28, 29, 3].

After the pioneering work of OSLSM [2], many few-shot segmentation methods have been proposed in the recent years [17, 18, 19, 20, 21, 22, 23, 24, 25, 26, 27, 1, 28, 29, 3]. Among others, an important challenge in few-shot segmentation is how to use support images to capture more meaningful information. Many recent state-of-the-art methods [1, 22, 23, 21, 30, 3] rely on feature masking (FM) [1] to discard irrelevant feature activations for reliable segmentation mask prediction. However, when masking a feature map, some crucial information in support images,

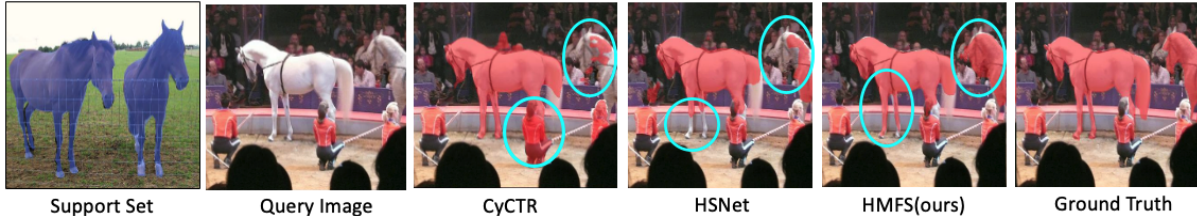


Figure 1: Compared to the current state-of-the-art methods [3] and [33], the proposed HMFS(ours) is capable of producing more accurate segmentation masks by recovering the fine-grained details (shown in cyan ellipse). For instance, observe the shirt of the person and the horse legs and its head.

such as the target object boundary, is partially lost. In particular, when the size of the target object is very small, this lost fine-grained spatial information makes it rather difficult to achieve accurate segmentation (see Fig. 1).

In this paper, we propose a simple, effective, and efficient way to enhance feature masking (FM). We dub the enhanced FM as hybrid masking. In particular, we compensate for the loss of target object details in FM technique through leveraging a simple input masking (IM) technique [2]. We note that IM is capable of preserving the fine details, especially around object boundaries, however, it lacks discriminative information, as such, after the removal of background information. To this end, we investigate the possibility of transferring object details in the IM to enrich FM technique. We instantiate the proposed hybrid masking (HM) into a recent strong baseline [3], and coin the resulting framework as HMFS. It produces more accurate segmentation masks by recovering the fine-grained details, such as target boundaries (see Fig. 1). Following are the main contributions of this paper:

- We propose a simple, effective and efficient way to enhance a de-facto feature masking technique (FM) in several recent few-shot segmentation methods.
- We perform extensive experiments to validate the effectiveness of proposed hybrid masking on three publicly available datasets: Pascal-5ⁱ [2], COCO-20ⁱ [31], and FSS-1000 [32]. Results show that the proposed HMFS approach outperforms the current state-of-the-art methods in all datasets. In particular, HMFS delivers an absolute gain of 3.6% and 5.9% over [33] with ResNet-50 and ResNet-101 [5] backbones, respectively under 1-shot setting on the challenging COCO-20ⁱ [31] dataset.
- We note that, the proposed HMFS approach improves training efficiency. Compared to baseline [3], it speeds up the training convergence up to 13x times on COCO-20ⁱ [31].

2 Related Work

Few-shot segmentation. The work of Shaban *et al.* [2] is believed to introduce the few shot segmentation task to the community. It generated segmentation parameters by using the conditioning branch on the support. Later, we have seen steady progress in this task, and so several methods were proposed [17, 18, 19, 20, 21, 22, 23, 24, 25, 26, 27, 1, 28, 29, 3]. CANet [22] modified the cosine similarity with the additive alignment module and enhanced the performance by performing iterations. To improve segmentation quality, PFENet [23] designed a pyramid module and used a prior map. Inspired by prototypical networks [34], PANet [21] leveraged novel prototype alignment network. Along similar lines, PPNet [35] utilized part-aware prototypes to get the detailed object features and PMM [19] used the expectation-maximization (EM) algorithm to generate multiple prototypes. ASGNet [29] proposed two modules, superpixel-guided clustering (SGC) and guided prototype allocation (GPC) to extract and allocate multiple prototypes. In pursuit of improving correspondence between support and query images, DAN [24] democratized the graph attention. Yang *et al.* [30] introduced a method to mine latent classes in the background, and CWT [28] designed simple classifier with transformer. CyCTR [33] mined information from the whole support image using transformer. Recently, HSNet [3] utilized efficient 4D convolution to analyze deeply accumulated features and achieved remarkable performance. We validate the effectiveness of our masking approach by instantiating it in the strong baseline method of HSNet [3].

Feature masking. Zhang *et al.* [1] proposed Masked Average Pooling (MAP) to eliminate irrelevant feature activations to facilitate reliable mask prediction, where feature masking (FM) was introduced and utilized before average pooling. Afterwards, FM was widely adopted as the de-facto technique to achieve feature masking [1, 22, 23, 21, 30, 3]. We note that, the FM method loses information about the target object in the process of feature masking. Specifically, it is prone to losing the fine-grained spatial details, which can be crucial towards generating precise segmentation mask. In this work, we compensate for the loss of target object details in FM technique via leveraging a simple input masking (IM) technique [2].

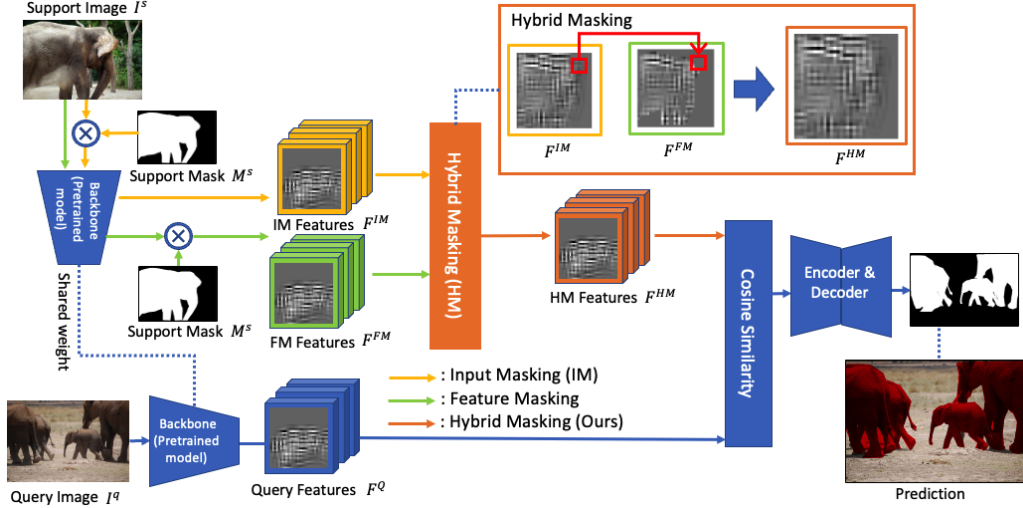


Figure 2: **The overall architecture of the proposed HMFS approach.** At its core, it contains a feature backbone, a feature masking (FM) technique, and an encoder/decoder. After extracting support and query features, the feature masking suppresses irrelevant activations in the support features. We introduce a simple, effective, and efficient way to enhance feature masking (FM), termed as hybrid masking (HM). It compensates for the loss of target object details in FM technique through leveraging a simple input masking (IM) technique [2].

Input masking. Input masking (IM) [2] is a technique to eliminate background pixels by multiplying the support image with its corresponding support mask. There were two key motivations behind erasing the background pixels. First, the network tends to be biased towards the largest object in the image, which may not be our target object to be segmented. Second, the variance of the output parameters will be increased by the background information. We observe that IM can preserve the fine details, however, it lacks target discriminative information, important for distinguishing between the foreground and the background. In this work, we investigate the possibility of transferring object details present in the IM to enrich the FM technique, thereby exploiting the complementary strengths of both.

3 Methodology

Fig. 2 displays the overall architecture of the proposed HMFS approach. Fundamentally, it comprises of a feature backbone for extracting support and query features, a feature masking (FM) technique for suppressing irrelevant support activations, and an encoder/decoder for predicting the segmentation mask from the relevant activations. In this work, we propose a simple, effective, and efficient way to enhance feature masking (FM), termed as hybrid masking (HM). It compensates for the loss of target object details in the FM technique by leveraging a simple input masking (IM) technique [2]. In what follows, we first layout the problem setting (sec. 3.1), next we describe feature masking technique (sec. 3.2), and finally we detail the proposed hybrid masking for few-shot segmentation (sec. 3.3).

3.1 Problem Setting

The goal of few-shot segmentation is to train a model capable of segmenting the target object in a query image given a few annotated images from the target class. We tackle this problem using the widely adopted episodic training scheme [36], which has been shown to reduce overfitting. Let us represent the disjoint sets of training and testing classes as C_{train} and C_{test} . The training data D_{train} belongs to C_{train} and the testing data D_{test} is from C_{test} . Multiple episodes are constructed using the D_{train} and D_{test} . Each episode consists of a support set, $S = (I^s, M^s)$, and a query set, $Q = (I^q, M^q)$, where I^* and M^* are an image and its mask. Namely, $D_{train} = \{(S_i, Q_i)\}_{i=1}^{N_{train}}$ and $D_{test} = \{(S_i, Q_i)\}_{i=1}^{N_{test}}$, where N_{train} and N_{test} denote the number of episodes for training and testing, respectively. During training, we iteratively sampled episodes from D_{train} to learn a mapping from (I^s, M^s, I^q) to query mask M^q . Afterwards, the learned model was evaluated without further optimization by randomly sampling episodes from the testing data D_{test} in the same manner and comparing the predicted query masks to the ground truth.

3.2 Feature Masking

Zhang *et al.* [1] argued that IM greatly increases the variance of the input data for a unified network, and according to Long *et al.* [37], the relative positions of input pixels can be preserved by fully convolutional networks. These two ideas motivated Masked Average Pooling (MAP), which ideally extracts the features of a target object while eliminating the background content. Although MAP falls short of this in practice, it remains helpful for learning better object features [11] while keeping the input structure of the network unchanged. In particular, the feature masking part is still widely used.

Given a support RGB image $I^s \in \mathbb{R}^{3 \times w \times h}$ and a support mask $M^s \in \{0, 1\}^{w \times h}$, where w and h are the width and height of the image, the support feature maps of I^s are $F^s \in \mathbb{R}^{c \times w' \times h'}$, where c is the number of channels, w' and h' are the width and height of the feature maps. Feature masking is performed after matching the mask to the feature size using the bilinear interpolation. We denote a function resizing the mask as $\tau(\cdot) : \mathbb{R}^{w \times h} \rightarrow \mathbb{R}^{c \times w' \times h'}$. Then, the feature masking features $F^{FM} \in \mathbb{R}^{c \times w' \times h'}$ are computed according to Eqn. 1,

$$F^{FM} = F^s \odot \tau(M^s), \quad (1)$$

where \odot denotes the Hadamard product. Zhang *et al.* [1] fit the feature size to the mask size, but we conversely fit the mask to the feature size.

Filter masking (FM), which is the core part of Masked Average Pooling (MAP) [1], is utilized to eliminate background information from support features and has become the de facto technique for masking feature maps, appearing in several recent few-shot segmentation methods [1, 22, 23, 21, 30] even in current state-of-the-art [3]. However, FM inadvertently eliminates both the background and the target object information because one pixel from the last layer's feature map corresponds to many pixels in the input image. Fig. 3 shows that the one pixel of the feature map could contain background and target object information together [38]. This is further analyzed in Fig. 6, which clearly shows that FM loses useful information through its masking and progressively worsens with deeper layers. If a target object in the support set appears very small, the segmentation of the query image becomes much more difficult because features are fed into network with relatively large proportion of undesired background features. Fig. 5 shows the limitation of FM.

3.3 Hybrid Masking for Few-shot Segmentation (HMFS)

We aim to achieve maximum cosine similarity between query features and support features so that the network can more accurately and efficiently learn to segment a target object.

The overall structure of the proposed method is shown in Fig. 2. We obtain two feature maps using IM and FM. Following the work of FPN [39, 3], we extract these features maps using deep convolutional layers and stack them to create 4D correlation tensors. We propose hybrid masking to merge these feature maps and find the correlation between the support features and query features using cosine similarity. This correlation set is fed into the encoder and the decoder, which takes full advantage of the given features to predict the target object mask.

Input Masking (IM). IM [2] eliminates background pixels by multiplying the support image with its corresponding support mask because of two empirical reasons. (1) The network tends to be biased towards the largest object in the image, which is not our target object to be segmented. (2) The variance of the output parameters will be increased by the background information.

Suppose we have the RGB support image $I^s \in \mathbb{R}^{3 \times w \times h}$ and a support mask $M^s \in \{0, 1\}^{w \times h}$ in the image space, where w and h are the width and height of the image. IM, computed as

$$I^{s'} = I^s \odot \tau(M^s), \quad (2)$$

contains the target object alone. We used the function $\tau(\cdot)$ for resizing the mask M^s to fit the image I^s .

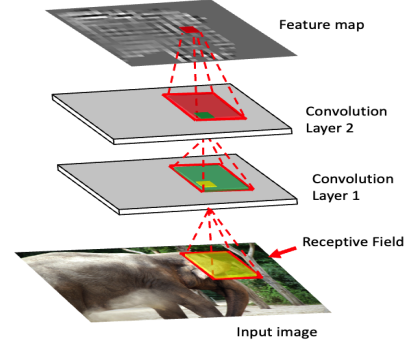


Figure 3: Receptive field analysis. The input image’s elephant is a target object and the other pixels are background. One pixel at the feature is generated from a lot of pixels’ information of previous pixels.

Hybrid Masking (HM). We propose an alternative masking approach, which takes advantage of the features generated by both FM and IM. First, FM and IM features are computed according to the existing methods. The unactivated values in the FM features are then replaced with IM features. Other activated values remain without replacing to maintain FM features. We name this process as hybrid masking (Alg. 1). HM prioritizes the information from FM features and supplements the lacking information, such as precise target boundaries, from IM features, which is superior for delineating the boundaries of target objects. The method is as follows even if feature maps are stacked to have a sequence of intermediate feature maps. Only one more loop is needed for the deep feature maps.

Algorithm 1: Hybrid Masking

Input : IM feature maps F^{IM} and FM features maps F^{FM}
Each channel $f_i^{IM} \in F^{IM}$ and $f_i^{FM} \in F^{FM}$
for $i = 1, c$ **do**
 Set $f_i^{HM} = f_i^{FM}$
 for Entire pixels $\in f_i^{HM}$ **do**
 Find a zero pixel $\in f_i^{HM}$
 if zero pixels found **then**
 Replace the zero pixel with corresponding pixels $\in f_i^{IM}$
 end
 end
end
Output : HM feature maps F^{HM}

3.3.1 Cosine similarity.

The cosine similarity is computed by comparing all pixel values between HM features and query features. Therefore, even if the position of the target object in the query image differs from the positions of target objects in the support set, the cosine similarity is unaffected. Suppose we have HM features $F^{HM} \in \mathbb{R}^{c \times w' \times h'}$ and query features $F^Q \in \mathbb{R}^{c \times w' \times h'}$. We resize and transpose these two features into $F^{HM'} \in \mathbb{R}^{c \times (w' \cdot h')}$ and $F^{Q'} \in \mathbb{R}^{(w' \cdot h') \times c}$, and construct the correlation set $C \in \mathbb{R}^{(w' \cdot h') \times (w' \cdot h')}$ as

$$C = ReLU \left(\frac{F^{Q'} \cdot F^{HM'}}{\|F^{Q'}\| \|F^{HM'}\|} \right). \quad (3)$$

Then, we resize again to get a 4D correlation set $C' \in \mathbb{R}^{w' \times h' \times w' \times h'}$.

3.3.2 Encoder and decoder.

For the last component, we adopted the encoder-decoder architecture used in HSNet [3], which reflects the recent state of the art. HSNet is best-suited for fully utilizing the features generated by hybrid masking, because it is able to analyze very deep features with efficient 4D convolutions. The 4D correlation set C' is fed into this last component.

4 Experiment

4.1 Setup

4.1.1 Datasets.

We evaluated the proposed method on three publicly available segmentation benchmarks: PASCAL-5ⁱ [2], COCO-20ⁱ [31], and FSS-1000 [32]. PASCAL-5ⁱ was created from PASCAL VOC 2012 [40] with extra mask annotations [41]. PASCAL-5ⁱ contains 20 types of object classes, COCO-20ⁱ contains 80 classes, and FSS-1000 contains 1000 classes. The PASCAL and COCO data sets were divided into four folds following training and evaluation methods of other works [35, 20, 23, 24, 19], where each fold of PASCAL-5ⁱ consisted of five classes, and each fold of COCO-20ⁱ had 20. We conducted cross-validation using these four folds. When evaluating a model on foldⁱ, all other classes not belonging to foldⁱ were used for training. 1000 episodes were sampled from foldⁱ to evaluate the trained model. For FSS-1000, the training, validation, and test datasets were divided into 520, 240, and 240 classes, respectively.

Table 1: Performance comparison with the existing methods on Pascal-5ⁱ [40]. Superscript asterisk denotes that data augmentation was applied during training.

Backbone feature	Methods	5 ⁰	5 ¹	5 ²	1-shot 5 ³	mIoU	FB-IoU	5 ⁰	5 ¹	5 ²	5-shot 5 ³	mIoU	FB-IoU
ResNet50 [5]	PANet [21]	44.0	57.5	50.8	44.0	49.1	-	55.3	67.2	61.3	53.2	59.3	-
	PFENet [23]	61.7	69.5	55.4	56.3	60.8	73.3	63.1	70.7	55.8	57.9	61.9	73.9
	ASGNet [29]	58.8	67.9	56.8	53.7	59.3	69.2	63.4	70.6	64.2	57.4	63.9	74.2
	CWT [28]	56.3	62.0	59.9	47.2	56.4	-	61.3	<u>68.5</u>	68.5	56.6	63.7	-
	RePRI [25]	59.8	68.3	62.1	48.5	59.7	-	64.6	<u>71.4</u>	71.1	59.3	66.6	-
	CyCTR [33]	<u>67.8</u>	72.8	58.0	58.0	64.2	-	71.1	73.2	60.5	57.5	65.6	-
	HSNet [3]	64.3	70.7	60.3	60.5	64.0	<u>76.7</u>	70.3	73.2	67.4	67.1	<u>69.5</u>	80.6
	HSNet* [3]	63.5	70.9	<u>61.2</u>	<u>60.6</u>	<u>64.3</u>	78.2	<u>70.9</u>	<u>73.1</u>	68.4	<u>65.9</u>	69.6	80.6
	HMFS*(ours)	69.0	<u>70.9</u>	59.3	61.0	65.0	76.5	69.9	72.0	63.4	63.3	67.1	<u>77.7</u>
ResNet101 [5]	FWB [20]	51.3	64.5	56.7	52.2	56.2	-	54.8	67.4	62.2	55.3	59.9	-
	DAN [24]	54.7	68.6	57.8	51.6	58.2	71.9	57.9	69.0	60.1	54.9	60.5	72.3
	PFENet [23]	60.5	69.4	54.4	55.9	60.1	72.9	62.8	70.4	54.9	57.6	61.4	73.5
	ASGNet [29]	59.8	67.4	55.6	54.4	59.3	71.7	64.6	71.3	64.2	57.3	64.4	75.2
	CWT [28]	56.9	65.2	61.2	48.8	58.0	-	62.6	70.2	68.8	57.2	64.7	-
	RePRI [25]	59.6	68.6	<u>62.2</u>	47.2	59.4	-	66.2	71.4	67.0	57.7	65.6	-
	CyCTR [33]	<u>69.3</u>	72.7	56.5	58.6	64.3	72.9	73.5	74.0	58.6	60.2	66.6	75.0
	HSNet [3]	67.3	<u>72.3</u>	62.0	63.1	<u>66.2</u>	77.6	71.8	<u>74.4</u>	67.0	<u>68.3</u>	70.4	80.6
	HSNet* [3]	67.5	72.7	63.5	<u>63.2</u>	66.7	<u>77.7</u>	71.7	74.8	<u>68.2</u>	68.7	70.8	80.9
	HMFS*(ours)	69.8	72.1	60.4	64.3	66.7	77.8	<u>72.2</u>	73.3	64.0	67.9	69.3	79.7

4.1.2 Implementation details.

We used ResNet50 [5] and ResNet101 [5] backbone networks pre-trained on ImageNet [42] with their weights frozen to extract features. From conv3_x to conv5_x of ResNet (i.e., the three layers before global average pooling), the features in the bottleneck part before the ReLU activation of each layer were stacked up to create deep features. We used the Adam optimizer [43] with learning rate 1e-3 and mini-batch size of 20 for all benchmarks. Following [44] and [45], we used data augmentation only for PASCAL-5ⁱ. For COCO-20ⁱ and FSS-1000 benchmarks, no data augmentation was employed.

4.1.3 Evaluation metrics.

Following [3, 23, 24], we adopt two evaluation metrics, mean intersection over union (mIoU) and foreground-background IoU (FB-IoU) for model evaluation. The mIoU averages the IoU values for all classes in each fold. FB-IoU calculates the foreground and background IoU values ignoring object classes and averages them. Note that, mIoU is a better indicator of model generalization than FB-IoU [3].

4.2 Comparison with the State-of-the-Art (SOTA)

4.2.1 PASCAL-5ⁱ.

Table 1 compares our method with other methods on PASCAL-5ⁱ datasets. In the 1-shot test, our method provides a gain of 0.7% mIoU compared to the state-of-the-art [3] with ResNet50 backbone. Our method performs on par with the existing best method of [3] with ResNet101. In the 5-shot test, our method shows slightly inferior performance in mIoU and FB-IoU.

4.2.2 COCO-20ⁱ.

Table 2 reports the results on the COCO-20ⁱ dataset. In the 1-shot test, our method shows a significant improvement over existing best method [3]; it delivers a gain of 3.6% and 5% in mIoU with ResNet50 and ResNet101 backbones, respectively. Similarly, in the 5-shot test, our method outperforms HSNet [3] by 3.4% and 1% with ResNet50 and ResNet101 backbones, respectively. Fig. 4 displays visual comparison with HSNet [3] under several challenging segmentation instances. We see that, compared to HSNet, the proposed approach produces more accurate segmentation masks that recover fine-grained details under appearance variations and complex backgrounds.

Table 2: Performance comparison on COCO-20ⁱ [31] in mIoU and FB-IoU with other methods. Best results are bold-faced.

Backbone feature	Methods	1-shot						5-shot					
		20 ⁰	20 ¹	20 ²	20 ³	mIoU	FB-IoU	20 ⁰	20 ¹	20 ²	20 ³	mIoU	FB-IoU
ResNet50 [5]	PMM [19]	29.3	34.8	27.1	27.3	29.6	-	33.0	40.6	30.3	33.3	34.3	-
	RPMM [19]	29.5	36.8	28.9	27.0	30.6	-	33.8	42.0	33.0	33.3	35.5	-
	PFENet [23]	36.5	38.6	34.5	33.8	35.8	-	36.5	43.3	37.8	38.4	39.0	-
	ASGNet [29]	-	-	-	-	34.6	60.4	-	-	-	-	42.5	67.0
	RePRI [25]	32.0	38.7	32.7	33.1	34.1	-	39.3	45.4	39.7	41.8	41.6	-
	HSNet [3]	36.3	<u>43.1</u>	38.7	38.7	39.2	<u>68.2</u>	<u>43.3</u>	<u>51.3</u>	<u>48.2</u>	<u>45.0</u>	<u>46.9</u>	<u>70.7</u>
	CyCTR [33]	<u>38.9</u>	43.0	<u>39.6</u>	<u>39.8</u>	<u>40.3</u>	-	41.1	48.9	45.2	47.0	45.6	-
	HMFS(ours)	39.3	45.7	46.9	43.7	43.9	70.8	43.8	53.1	52.1	47.0	49.0	72.2
ResNet101 [5]	FWB [20]	17.0	18.0	21.0	28.9	21.2	-	19.1	21.5	23.9	30.1	23.7	-
	DAN [24]	-	-	-	-	24.4	62.3	-	-	-	-	29.6	63.9
	PFENet [23]	<u>36.8</u>	41.8	<u>38.7</u>	36.7	38.5	63.0	40.4	46.8	43.2	40.5	42.7	65.8
	HSNet [3]	37.2	<u>44.1</u>	<u>42.4</u>	<u>41.3</u>	<u>41.2</u>	<u>69.1</u>	<u>45.9</u>	<u>53.0</u>	<u>51.8</u>	<u>47.1</u>	<u>49.5</u>	<u>72.4</u>
	HMFS(ours)	40.0	50.0	48.8	45.9	46.2	71.5	45.9	55.2	51.8	48.9	50.5	72.9

Table 3: Performance comparison with other methods on FSS-1000 [32] dataset. Best results are bold-faced.

Backbone feature	Methods	mIoU		Backbone feature	Methods	mIoU	
		1-shot	5-shot			1-shot	5-shot
ResNet50	FSOT	82.5	83.8	ResNet101	DAN	85.2	88.1
	HSNet	<u>85.5</u>	<u>87.8</u>		HSNet	<u>86.5</u>	88.5
	HMFS (ours)	87.1	88.0		HMFS (ours)	87.8	88.5

4.2.3 FSS-1000.

Table 3 compares our proposed method and the other methods on the FSS-1000 dataset. In the 1-shot test, our method yields a gain of 1.6% and 1.3% in mIoU over [3] with ResNet50 and ResNet101 backbones, respectively. In the 5-shot test, we observe an improvement of 0.2% in mIoU over [3] with the ResNet50 backbone.

4.2.4 Generalization test.

Following previous works [3, 25], we perform a domain shift test to evaluate the generalization capability of the proposed method. We trained a model on the COCO-20ⁱ dataset and tested this model on the PASCAL-5ⁱ dataset. The training/testing folds were constructed following [25, 3]. The objects in training classes did not overlap with object in the testing classes. As shown in Table 4, our method outperforms the current state-of-the-art approaches under both 1-shot and 5-shot test. In 1-shot test, it delivers a 2% mIoU gain over RePRI[25] and a 2.4% mIoU gain over HSNet[3] with ResNet50 and ResNet101 backbones, respectively. In the 5-shot test, our method outperforms HSNet[3] by 1.0% and 0.6% in mIoU with ResNet50 and ResNet101 backbones, respectively.

4.3 Ablation Study and Analysis

4.3.1 Comparison of the three different masking approaches.

We compare all three masking approaches, IM [2], FM [1], and the proposed HM after incorporating them into HSNet [3] and evaluating them on the COCO-20ⁱ dataset (Table 5). We can see that in both 1-shot and 5-shot tests, the proposed HM approach provides noticeable gains over either individual FM and IM techniques. Particularly, in 1-shot test with ResNet50 backbone, the proposed hybrid masking (HM) delivers a gain of 1.4% over IM.

Fig. 5 shows the qualitative results from the three masking methods. The blue objects in the support set are the target objects for segmentation. The red pixels are the segmentation results. FM can coarsely segment the objects from the background but fails to precisely recover target details, such as target boundaries. IM is capable of recovering precise object boundaries, but struggles in distinguishing objects from the background. The proposed approach, HM, clearly distinguishes between the target objects and the background and also recovers precise details such as, target boundaries.

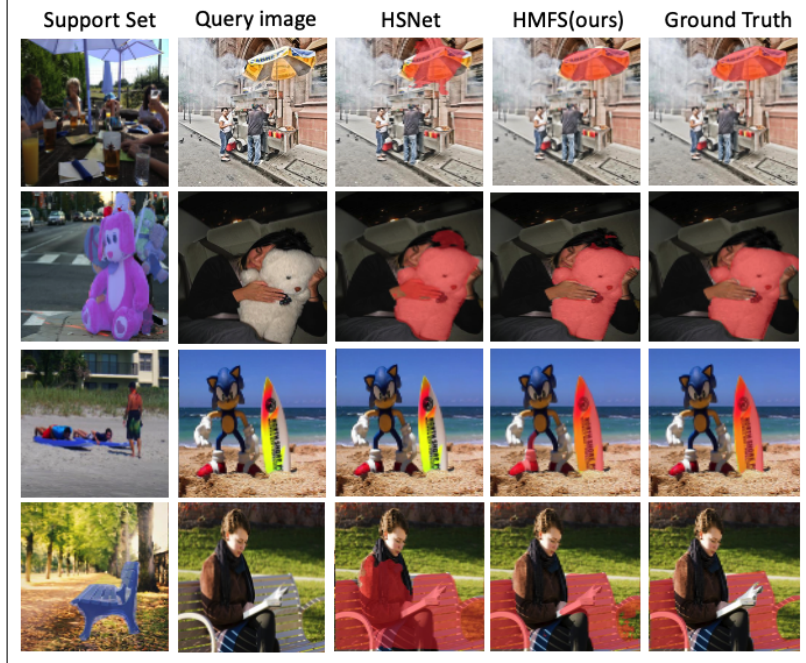


Figure 4: **Visual comparison with HSNet [3] under several challenging segmentation instances from COCO-20ⁱ [31] dataset.** Compared to HSNet, the proposed approach produces more accurate segmentation masks that also recover fine-grained details under various appearance variations and complex backgrounds.

Table 4: Comparison of generalization performance with domain shift test. A model was trained on COCO-20ⁱ [31] and then evaluated on PASCAL-5ⁱ [40].

Backbone feature	Methods	1-shot					5-shot				
		5 ⁰	5 ¹	5 ²	5 ³	mIoU	5 ⁰	5 ¹	5 ²	5 ³	mIoU
ResNet50 [5]	RPM [19]	36.3	55.0	52.5	54.6	49.6	40.2	58.0	55.2	61.8	53.8
	PFENet [23]	43.2	<u>65.1</u>	<u>66.5</u>	69.7	61.1	45.1	66.8	68.5	73.1	63.4
	RePRI [25]	52.2	64.3	64.8	71.6	<u>63.2</u>	<u>56.5</u>	<u>68.2</u>	70.0	76.2	67.7
	HSNet [3]	<u>45.4</u>	61.2	63.4	<u>75.9</u>	61.6	56.9	65.9	<u>71.3</u>	<u>80.8</u>	<u>68.7</u>
	HMFS(ours)	43.4	68.2	69.4	79.9	65.2	50.7	71.4	73.4	83.1	69.7
ResNet101 [5]	HSNet [3]	<u>47.0</u>	<u>65.2</u>	<u>67.1</u>	<u>77.1</u>	<u>64.1</u>	57.2	<u>69.5</u>	<u>72.0</u>	<u>82.4</u>	<u>70.3</u>
	HMFS(ours)	46.7	68.6	71.1	79.7	66.5	<u>53.7</u>	70.7	75.2	83.9	70.9

Table 5: **Ablation study of the three different masking methods on COCO-20ⁱ [31].**

Backbone feature	Masking methods	1-shot						5-shot					
		20 ⁰	20 ¹	20 ²	20 ³	mIoU	FB-IoU	20 ⁰	20 ¹	20 ²	20 ³	mIoU	FB-IoU
ResNet50 [5]	FM [1]	36.3	43.1	38.7	38.7	39.2	68.2	43.3	<u>51.3</u>	48.2	45.0	46.9	70.7
	IM [2]	39.8	<u>45.0</u>	<u>46.0</u>	<u>43.2</u>	<u>43.5</u>	<u>70.0</u>	<u>43.4</u>	50.9	<u>49.5</u>	48.0	<u>47.6</u>	<u>71.7</u>
	HM(ours)	<u>39.3</u>	45.7	46.9	43.7	43.9	70.8	43.8	53.1	52.1	<u>47.0</u>	49.0	72.2
ResNet101 [5]	FM [1]	37.2	44.1	42.4	41.3	41.2	69.1	<u>45.9</u>	53.0	51.8	47.1	49.5	72.4
	IM [2]	41.0	<u>48.3</u>	<u>47.3</u>	<u>44.5</u>	<u>45.2</u>	<u>70.9</u>	46.6	<u>54.5</u>	<u>50.4</u>	<u>47.7</u>	<u>49.8</u>	<u>72.7</u>
	HM(ours)	<u>40.0</u>	50.0	48.8	45.9	46.2	71.5	<u>45.9</u>	55.2	51.8	48.9	50.5	72.9

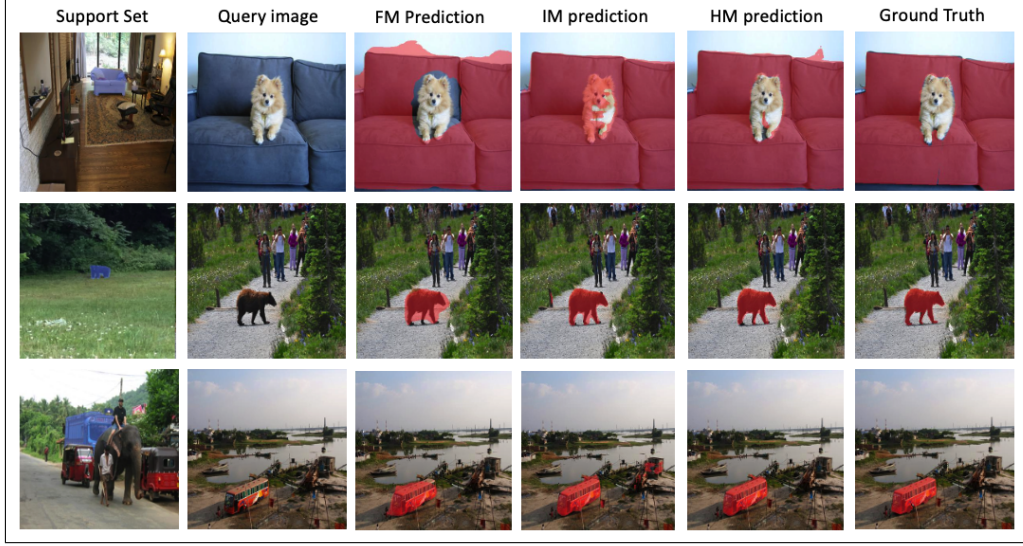


Figure 5: **Qualitative comparison of three different masking approaches on COCO-20¹⁷ [31].** The blue objects in the support set are the target objects for segmentation. The red pixels are the segmentation results. FM can coarsely segment the objects from the background but fails to precisely recover target details, such as target boundaries. IM is capable of recovering precise object boundaries, but struggles in distinguishing objects from the background. The proposed approach, HM, clearly distinguishes between the target objects and the background and also recovers precise details such as, target boundaries.

Fig. 6 shows the visual comparison between the feature maps of IM and FM features. The feature maps inside the red rectangles reveal that the two features produced from the two masking approaches are different. Looking at the area where activations occur in the IM feature map at layer 50, we can see it is more indicative of the target object boundaries than the FM feature. Additionally, looking at the IM feature map at layer 34, we observe that there is a strong signal around the edge of the target object. This happens because FM performs masking after getting features. This results in less precise target boundaries.

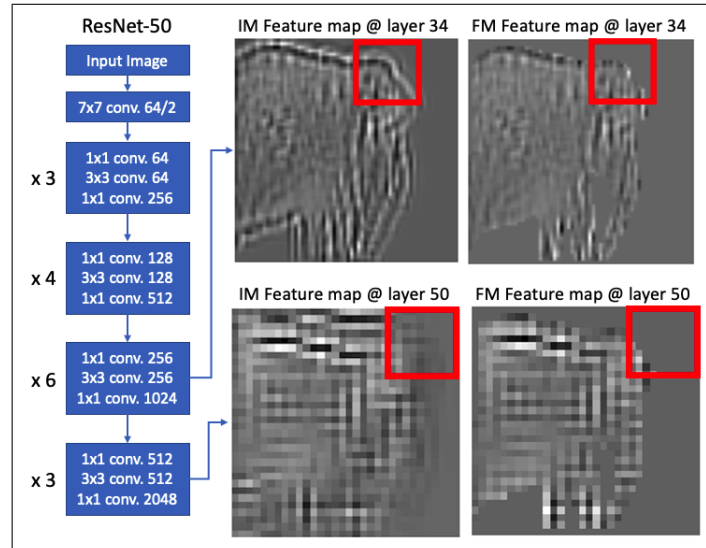


Figure 6: Visual comparison between the feature maps of IM and FM. These are from ResNet50 at layer34 and layer50. We visualize the first channel of the feature map in grayscale. The feature maps inside the red rectangles reveal that the features from the two feature masking methods are different. Observe activations in the IM feature map at layer 50, it is more indicative of the target object boundaries than the FM feature. Additionally, the IM feature map at layer 34 displays a strong signal around the edge of the target object.

Training efficiency. Fig. 7 shows the training profiles of HSNet[3] and HMFS on COCO-20ⁱ. It is apparent that HMFS is capable of achieving faster training convergence in comparison to HSNet due to the proposed hybrid masking (HM) technique. More precisely, HMFS provides approximately 13x faster convergence compared to HSNet. A similar trend was observed on the PASCAL-5ⁱ and FSS-1000 datasets, for which the results are reported in the supplementary materials.

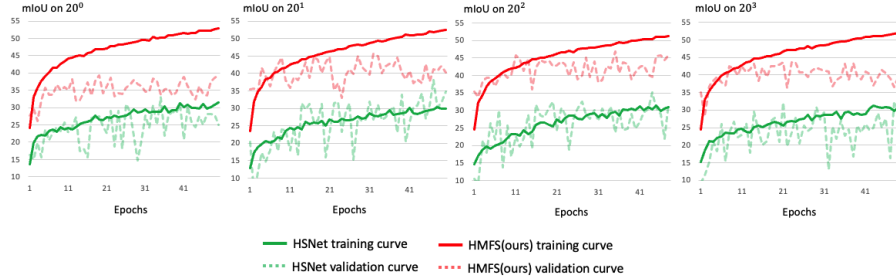


Figure 7: Training profiles of HSNet[3] and HMFS(Ours) on COCO-20ⁱ.

Runtime comparison. Since the hybrid addition takes an additional pass over the pixel values to choose between FM and IM, there may be concerns about the calculation speed. We measured the computation time of the HM method and other methods for comparison. Although the computation time of the HM method increased by 40% compared to other methods, resulting in 0.07 images/s, we believe that the $\sim 1300\%$ improvement in convergence speed is a worthwhile trade-off. This high speed was possible due to PyTorch’s GPU parallel processing [46].

Limitations. We notice that the performance of proposed HMFS can be further improved on the PASCAL-5ⁱ [40] dataset. We found that HMFS performance in PASCAL-5ⁱ [40] was inferior to the performance of the COCO-20ⁱ [31] dataset. A potential reason is that HMFS quickly enters the over-fitting phase due to abundance of information about the target object. The following data augmentation method [44, 45] was able to alleviate this problem to some extent, but it did not solve the problem completely. Further, we identify some failure cases for HMFS (Fig. 8). Our method struggles when the target is occluded due to small objects. Also, when the appearance/shape of the target image of the support set and the target image of the query image is radically different.



Figure 8: Although HMFS improves mIoU compared to other methods, its performance can be further improved. We identify cases where HMFS struggles to produce accurate segmentation masks (shown as a cyan ellipse).

5 Conclusion

We proposed a new masking approach, termed as hybrid masking. It aims to enhance FM, that is commonly used in existing SOTA methods. We instantiate HM in a strong baseline, and term it as HMFS. Results reveal that HMFS surpasses the existing SOTA by visible margins and also improves training efficiency.

References

- [1] Xiaolin Zhang, Yunchao Wei, Yi Yang, and Thomas Huang. Sg-one: Similarity guidance network for one-shot semantic segmentation. *IEEE Transactions on Cybernetics*, 50:3855–3865, 2020.
- [2] Amirreza Shaban, Shray Bansal, Zhen Liu, Irfan Essa, and Byron Boots. One-shot learning for semantic segmentation. In Gabriel Brostow Tae-Kyun Kim, Stefanos Zafeiriou and Krystian Mikolajczyk, editors, *Proceedings of the British Machine Vision Conference (BMVC)*, pages 167.1–167.13. BMVA Press, September 2017.
- [3] Juhong Min, Dahyun Kang, and Minsu Cho. Hypercorrelation squeeze for few-shot segmentation. In *Proceedings of the IEEE/CVF International Conference on Computer Vision (ICCV)*, pages 6941–6952, October 2021.
- [4] Alex Krizhevsky, Ilya Sutskever, and Geoffrey E Hinton. Imagenet classification with deep convolutional neural networks. *Advances in Neural Information Processing Systems*, 25, 2012.
- [5] Kaiming He, Xiangyu Zhang, Shaoqing Ren, and Jian Sun. Deep residual learning for image recognition. In *2016 IEEE Conference on Computer Vision and Pattern Recognition (CVPR)*, pages 770–778. IEEE Computer Society, 2016.
- [6] Karen Simonyan and Andrew Zisserman. Very deep convolutional networks for large-scale image recognition. In Yoshua Bengio and Yann LeCun, editors, *3rd International Conference on Learning Representations, ICLR 2015, San Diego, CA, USA, May 7-9, 2015, Conference Track Proceedings*, 2015.
- [7] Gao Huang, Zhuang Liu, Laurens Van Der Maaten, and Kilian Q Weinberger. Densely connected convolutional networks. In *Proceedings of the IEEE Conference on Computer Vision and Pattern Recognition (CVPR)*, pages 4700–4708, 2017.
- [8] Shaoqing Ren, Kaiming He, Ross Girshick, and Jian Sun. Faster r-cnn: Towards real-time object detection with region proposal networks. *Advances in neural information processing systems*, 28, 2015.
- [9] Joseph Redmon, Santosh Divvala, Ross Girshick, and Ali Farhadi. You only look once: Unified, real-time object detection. In *Proceedings of the IEEE conference on computer vision and pattern recognition (CVPR)*, pages 779–788, 2016.
- [10] Wei Liu, Dragomir Anguelov, Dumitru Erhan, Christian Szegedy, Scott Reed, Cheng-Yang Fu, and Alexander C Berg. Ssd: Single shot multibox detector. In *European conference on computer vision*, pages 21–37. Springer, 2016.
- [11] Liang-Chieh Chen, George Papandreou, Iasonas Kokkinos, Kevin Murphy, and Alan L. Yuille. Deeplab: Semantic image segmentation with deep convolutional nets, atrous convolution, and fully connected crfs. *IEEE Transactions on Pattern Analysis and Machine Intelligence*, 40(4):834–848, 2018.
- [12] J. Long, E. Shelhamer, and T. Darrell. Fully convolutional networks for semantic segmentation. In *2015 IEEE Conference on Computer Vision and Pattern Recognition (CVPR)*, pages 3431–3440, Los Alamitos, CA, USA, jun 2015. IEEE Computer Society.
- [13] Hengshuang Zhao, Jianping Shi, Xiaojuan Qi, Xiaogang Wang, and Jiaya Jia. Pyramid scene parsing network. In *2017 IEEE Conference on Computer Vision and Pattern Recognition (CVPR)*, pages 6230–6239, 2017.
- [14] Zilong Huang, Xinggang Wang, Jiasi Wang, Wenyu Liu, and Jingdong Wang. Weakly-supervised semantic segmentation network with deep seeded region growing. In *2018 IEEE/CVF Conference on Computer Vision and Pattern Recognition (CVPR)*, pages 7014–7023, 2018.
- [15] Yunchao Wei, Huaxin Xiao, Honghui Shi, Zequn Jie, Jiashi Feng, and Thomas S. Huang. Revisiting dilated convolution: A simple approach for weakly- and semi-supervised semantic segmentation. In *Proceedings of the IEEE Conference on Computer Vision and Pattern Recognition (CVPR)*, June 2018.
- [16] Y. Wei, J. Feng, X. Liang, M. Cheng, Y. Zhao, and S. Yan. Object region mining with adversarial erasing: A simple classification to semantic segmentation approach. In *2017 IEEE Conference on Computer Vision and Pattern Recognition (CVPR)*, pages 6488–6496, Los Alamitos, CA, USA, jul 2017. IEEE Computer Society.
- [17] Kate Rakelly, Evan Shelhamer, Trevor Darrell, Alyosha A. Efros, and Sergey Levine. Conditional networks for few-shot semantic segmentation. In *6th International Conference on Learning Representations, ICLR 2018, Vancouver, BC, Canada, April 30 - May 3, 2018, Workshop Track Proceedings*. OpenReview.net, 2018.
- [18] Mennatullah Siam, Boris N. Oreshkin, and Martin Jägersand. AMP: adaptive masked proxies for few-shot segmentation. In *2019 IEEE/CVF International Conference on Computer Vision, ICCV 2019, Seoul, Korea (South), October 27 - November 2, 2019*, pages 5248–5257. IEEE, 2019.
- [19] Boyu Yang, Chang Liu, Bohao Li, Jianbin Jiao, and Ye Qixiang. Prototype mixture models for few-shot semantic segmentation. In *ECCV*, 2020.

- [20] Khoi Nguyen and Sinisa Todorovic. Feature weighting and boosting for few-shot segmentation. In *Proceedings of the IEEE/CVF International Conference on Computer Vision (ICCV)*, October 2019.
- [21] Kaixin Wang, Jun Hao Liew, Yingtian Zou, Daquan Zhou, and Jiashi Feng. Panet: Few-shot image semantic segmentation with prototype alignment. In *The IEEE International Conference on Computer Vision (ICCV)*, October 2019.
- [22] Chi Zhang, Guosheng Lin, Fayao Liu, Rui Yao, and Chunhua Shen. Canet: Class-agnostic segmentation networks with iterative refinement and attentive few-shot learning. In *Proceedings of the IEEE/CVF Conference on Computer Vision and Pattern Recognition (CVPR)*, June 2019.
- [23] Zhuotao Tian, Hengshuang Zhao, Michelle Shu, Zhicheng Yang, Ruiyu Li, and Jiaya Jia. Prior guided feature enrichment network for few-shot segmentation. *TPAMI*, 2020.
- [24] Haochen Wang, Xudong Zhang, Yutao Hu, Yandan Yang, Xianbin Cao, and Xiantong Zhen. Few-shot semantic segmentation with democratic attention networks. In Andrea Vedaldi, Horst Bischof, Thomas Brox, and Jan-Michael Frahm, editors, *Computer Vision – ECCV 2020*, pages 730–746, Cham, 2020. Springer International Publishing.
- [25] Malik Boudiaf, Hoel Kervadec, Ziko Imtiaz Masud, Pablo Piantanida, Ismail Ben Ayed, and Jose Dolz. Few-shot segmentation without meta-learning: A good transductive inference is all you need? In *Proceedings of the IEEE/CVF Conference on Computer Vision and Pattern Recognition (CVPR)*, pages 13979–13988, June 2021.
- [26] Guo-Sen Xie, Jie Liu, Huan Xiong, and Ling Shao. Scale-aware graph neural network for few-shot semantic segmentation. In *Proceedings of the IEEE/CVF Conference on Computer Vision and Pattern Recognition (CVPR)*, pages 5475–5484, June 2021.
- [27] Weide Liu, Chi Zhang, Henghui Ding, Tzu-Yi Hung, and Guosheng Lin. Few-shot segmentation with optimal transport matching and message flow. *ArXiv*, abs/2108.08518, 2021.
- [28] Zhihe Lu, Sen He, Xiatian Zhu, Li Zhang, Yi-Zhe Song, and Tao Xiang. Simpler is better: Few-shot semantic segmentation with classifier weight transformer. In *ICCV*, 2021.
- [29] Gen Li, Varun Jampani, Laura Sevilla-Lara, Deqing Sun, Jonghyun Kim, and Joongkyu Kim. Adaptive prototype learning and allocation for few-shot segmentation. In *CVPR*, 2021.
- [30] Lihe Yang, Wei Zhuo, Lei Qi, Yinghuan Shi, and Yang Gao. Mining latent classes for few-shot segmentation. In *ICCV*, 2021.
- [31] Tsung-Yi Lin, Michael Maire, Serge Belongie, Lubomir Bourdev, Ross Girshick, James Hays, Pietro Perona, Deva Ramanan, C. Lawrence Zitnick, and Piotr Dollár. Microsoft coco: Common objects in context, 2015.
- [32] Xiang Li, Tianhan Wei, Yau Pun Chen, Yu-Wing Tai, and Chi-Keung Tang. Fss-1000: A 1000-class dataset for few-shot segmentation. *CVPR*, 2020.
- [33] Gengwei Zhang, Guoliang Kang, Yi Yang, and Yunchao Wei. Few-shot segmentation via cycle-consistent transformer, 2021.
- [34] Jake Snell, Kevin Swersky, and Richard Zemel. Prototypical networks for few-shot learning. *Advances in neural information processing systems*, 30, 2017.
- [35] Yongfei Liu, Xiangyi Zhang, Songyang Zhang, and Xuming He. Part-aware prototype network for few-shot semantic segmentation, 2020.
- [36] Oriol Vinyals, Charles Blundell, Timothy Lillicrap, koray kavukcuoglu, and Daan Wierstra. Matching networks for one shot learning. In D. Lee, M. Sugiyama, U. Luxburg, I. Guyon, and R. Garnett, editors, *Advances in Neural Information Processing Systems*, volume 29. Curran Associates, Inc., 2016.
- [37] J. Long, E. Shelhamer, and T. Darrell. Fully convolutional networks for semantic segmentation. In *2015 IEEE Conference on Computer Vision and Pattern Recognition (CVPR)*, pages 3431–3440, Los Alamitos, CA, USA, jun 2015. IEEE Computer Society.
- [38] Wenjie Luo, Yujia Li, Raquel Urtasun, and Richard Zemel. Understanding the effective receptive field in deep convolutional neural networks. In *Proceedings of the 30th International Conference on Neural Information Processing Systems, NIPS’16*, page 4905–4913, Red Hook, NY, USA, 2016. Curran Associates Inc.
- [39] T. Lin, P. Dollar, R. Girshick, K. He, B. Hariharan, and S. Belongie. Feature pyramid networks for object detection. In *2017 IEEE Conference on Computer Vision and Pattern Recognition (CVPR)*, pages 936–944, Los Alamitos, CA, USA, jul 2017. IEEE Computer Society.
- [40] Mark Everingham, Luc Van Gool, Christopher Williams, John Winn, and Andrew Zisserman. The pascal visual object classes (voc) challenge. *International Journal of Computer Vision*, 88:303–338, 06 2010.

- [41] Bharath Hariharan, Pablo Arbeláez, Ross Girshick, and Jitendra Malik. Simultaneous detection and segmentation. In David Fleet, Tomas Pajdla, Bernt Schiele, and Tinne Tuytelaars, editors, *Computer Vision – ECCV 2014*, pages 297–312, Cham, 2014. Springer International Publishing.
- [42] Jia Deng, Wei Dong, Richard Socher, Li-Jia Li, Kai Li, and Li Fei-Fei. Imagenet: A large-scale hierarchical image database. In *2009 IEEE Conference on Computer Vision and Pattern Recognition (CVPR)*, pages 248–255, 2009.
- [43] Diederik P. Kingma and Jimmy Ba. Adam: A method for stochastic optimization. In Yoshua Bengio and Yann LeCun, editors, *3rd International Conference on Learning Representations, ICLR 2015, San Diego, CA, USA, May 7-9, 2015, Conference Track Proceedings*, 2015.
- [44] Alexander Buslaev, Vladimir Iglovikov, Eugene Khvedchenya, Alex Parinov, Mikhail Druzhinin, and Alexandr Kalinin. Albumentations: Fast and flexible image augmentations. *Information*, 11:125, 02 2020.
- [45] Seokju Cho, Sunghwan Hong, Sangryul Jeon, Yunsung Lee, Kwanghoon Sohn, and Seungryong Kim. Cats: Cost aggregation transformers for visual correspondence. In *Thirty-Fifth Conference on Neural Information Processing Systems*, 2021.
- [46] Adam Paszke, Sam Gross, Francisco Massa, Adam Lerer, James Bradbury, Gregory Chanan, Trevor Killeen, Zeming Lin, Natalia Gimelshein, Luca Antiga, Alban Desmaison, Andreas Köpf, Edward Yang, Zach DeVito, Martin Raison, Alykhan Tejani, Sasank Chilamkurthy, Benoit Steiner, Lu Fang, Junjie Bai, and Soumith Chintala. *PyTorch: An Imperative Style, High-Performance Deep Learning Library*. Curran Associates Inc., Red Hook, NY, USA, 2019.